Published in final edited form as:

Neuroscience. 2019 November 10; 420: 97–111. doi:10.1016/j.neuroscience.2018.12.045.

The SNAP25 Interactome in Ventromedial Caudate in Schizophrenia Includes the Mitochondrial Protein ARF1

Alfredo Ramos-Miguel[a,b,c,†], **Vilte Barakauskas**[a,d,†], **Jehan Alamri**[a], **Masatoshi Miyauchi**[a,b], **Alasdair M. Barr**[a,e], **Clare L. Beasley**[a,b], **Gorazd Rosoklija**[f], **J. John Mann**[f], **Andrew J. Dwork**[f], **Annie Moradian**[g], **Gregg B. Morin**[g], **William G. Honer**[a,b,*]

[a]BC Mental Health and Addictions Research Institute, 938 West 28th Ave, Vancouver, BC V5Z 4H4, Canada

[b]Department of Psychiatry, University of British Columbia, 2255 Wesbrook Mall, Vancouver, BC V6T 2A1, Canada

[c]Department of Pharmacology, University of the Basque Country, Centro de Investigación Biomédica en Red de Salud Mental, CIBERSAM, Barrio Sarriena, s/n, 48940 Leioa, Biscay, Spain

[d]Department of Pathology and Laboratory Medicine, University of British Columbia, 2J9-4500 Oak St., Vancouver, BC V6H 3B1, Canada

[e]Department of Anesthesiology, Pharmacology, & Therapeutics, University of British Columbia, 2176 Health Sciences Mall Vancouver, BC V6T 1Z3, Canada

[f]Department of Psychiatry, Columbia University, 1051 Riverside Drive, New York, NY 10032, USA

[g]Department of Medical Genetics, University of British Columbia, C234-4500 Oak St., Vancouver, BC V6H 3B1, Canada

Abstract

Abnormalities of SNAP25 (synaptosome-associated protein 25) amount and protein-protein interactions occur in schizophrenia, and may contribute to abnormalities of neurotransmitter release in patients. However, presynaptic terminal function depends on multiple subcellular mechanisms, including energy provided by mitochondria. To explore the SNAP25 interactome in schizophrenia, we immunoprecipitated SNAP25 along with interacting proteins from the ventromedial caudate of 15 cases of schizophrenia and 13 controls. Proteins were identified with mass spectrometry-based proteomics. As well as 15 SNARE- (soluble N-ethylmaleimide-sensitive factor attachment protein receptor) associated proteins, we identified 17 mitochondria-associated and four other proteins. The mitochondrial small GTPase ARF1 (ADP-ribosylation factor 1) was identified in eight schizophrenia SNAP25 immunoprecipitates and none from controls ($P = 0.004$).

*Correspondence to: W. G. Honer, Department of Psychiatry, University of British Columbia, 2255 Wesbrook Mall, Vancouver, BC V6T 2A1, Canada. william.honer@ubc.ca (W. G. Honer).
†Both these authors contributed equally to the manuscript.

DECLARATION OF INTEREST

WGH has received consulting fees or sat on advisory boards for: In Silico, Lundbeck/Otsuka, Alphasights and Newron. AMB is on the advisory board or received consulting fees from Roche Canada, and received educational grant support from BMS Canada. The organizations cited above had no role in (and therefore did not influence) the design of the present study, the interpretation of results, and/or preparation of the manuscript. Other authors do not have any financial disclosures to report.

Although the ARF1-SNAP25 interaction may be increased, immunoblotting demonstrated 21% lower ARF1–21 (21 kiloDaltons) in schizophrenia samples ($P = 0.04$). In contrast, the mitochondrial protein UQCRC1 (ubiquinol-cytochrome c reductase core protein 1) did not differ. Lower ARF1–21 levels were associated with the previously reported increased SNAP25-syntaxin interaction in schizophrenia ($r = 0.39$, $P = 0.04$). Additional immunoprecipitation studies confirmed the ARF1–21-SNAP25 interaction, independent of UQCRC1. Both ARF1 and SNAP25 were localized to synaptosomes. Confocal microscopy demonstrated co-localization of ARF1 and SNAP25, and further suggested fivefold enrichment of ARF1 in synaptosomes containing an excitatory marker (vesicular glutamate transporter) compared with synaptosomes containing an inhibitory marker (vesicular GABA transporter). The present findings suggest an association between abnormalities of SNARE proteins involved with vesicular neurotransmission and the mitochondrial protein ARF1 that may contribute to the pathophysiology of schizophrenia.

Keywords

schizophrenia; postmortem brain; presynaptic; mitochondria; proteomics

INTRODUCTION

The pathophysiology of schizophrenia includes presynaptic mechanisms governing neurotransmitter release, as well as postsynaptic mechanism related to receptors and signaling pathways. The striatum is an important target for studies of these mechanisms (Perez-Costas et al., 2010). Striatal dopamine release in increased in the prodromal and acute phases of illness, and in patients who respond to antipsychotic drugs compared with those who do not (Abi-Dargham et al., 2009; Howes et al., 2009; Kegeles et al., 2010; Demjaha et al., 2012, 2014). As a potential correlate, studies of striatum using electron microscopy indicate greater numbers of corticostriatal synapses in anterior caudate in schizophrenia (Roberts et al., 2005, 2008).

Examination of presynaptic proteins in postmortem tissue allows characterization of the molecular abnormalities that may contribute to the findings in patients. In the ventromedial caudate (part of the associative striatum) we reported lower levels of SNAP25 and syntaxin in schizophrenia, with similar but smaller changes in the nucleus accumbens, and no differences in the dorsal caudate (Barakauskas et al., 2010). Examination of subregional variation in schizophrenia may have contributed to these findings, in contrast to another study where overall striatal levels of SNAP25 were found to be unchanged (Dean et al., 2015). Differences in SNARE protein amount alone may not be central to the mechanism of illness, instead, interactions between the proteins may be more important (Katrancha and Koleske, 2015). In the same samples with low SNAP25 and syntaxin in ventromedial caudate, we observed increased SNAP25-syntaxin protein-protein interaction (Barakauskas et al., 2010). Subsequently, increased SNARE complex formation in orbitofrontal cortex was reported in this series of samples, and in a replication series (Ramos-Miguel et al., 2015a). The orbitofrontal cortex study used non-denaturing gel electrophoresis, allowing identification of multiple protein complexes containing canonical SNARE proteins as well as other partners. In an animal model with increased SNARE protein-protein interaction due

to a mutation in SNAP25, interesting phenotypic similarities with some aspects of schizophrenia were reported (Jeans et al., 2007; Oliver and Davies, 2009; Oliver et al., 2012).

More detailed characterization of the diversity of protein content of synapses may allow identification of disease-related targets. The protein composition of rodent synapses was described in detail by using a fractionation protocol followed by proteomics (Wilhelm et al., 2014). Protein-protein interactions in presynaptic terminals can be investigated by a range of techniques (Laßek et al., 2015). Once an illness-associated target protein is identified, broader investigation of potential interacting partners using immunoprecipitation of the target followed by mass spectrometry to identify potential binding partners can be a fruitful strategy (Martins-de-Souza et al., 2015). By first isolating cortical membranes, then immunoprecipitating with an antibody reactive with SNAP25, followed by mass spectrometry, multiple SNAP25 interacting proteins were described (Gorini et al., 2010). These included the expected interacting SNARE proteins syntaxin-1A and VAMP, as well as a host of novel interacting partners. An analogous study was carried out using human brain homogenates, with SNAP25 immunoprecipitation followed by mass spectrometry (Brinkmalm et al., 2014). While the focus of the latter study was measuring the amounts of co-immunoprecipitated syntaxin and VAMP in control and Alzheimer's disease samples, multiple other interacting proteins were identified. The co-immunoprecipitated proteins included mitochondrial and other proteins involved with the high metabolic demand in synapses (SaiaCereda and Martins-de-Souza, 2017). Studies with electron microscopy in (understandably) small numbers of cases indicate fewer synaptic mitochondria in treatment responsive schizophrenia, but unchanged numbers in treatment resistant (Roberts, 2017). Mitochondria are dynamic. According to tissue energy demands and stress responses, mitochondria may undergo fission (increasing copy number) or fusion (decreasing copy number). In schizophrenia, mitochondrial hyperplasia occurs in terminals contacting dopaminergic neurons (Roberts, 2017).

Non-denaturing, blue-native gels allowed targeted exploration of the SNAP25 interactome in schizophrenia, and in patients with age-related cognitive impairment (Ramos-Miguel et al., 2015a, 2018). The present study was designed to use immunoprecipitation followed by mass spectrometry to assess the SNAP25 interactome in the same series of cases and controls where greater SNARE complex interactions were described in schizophrenia. Enough tissue from the ventromedial caudate was available to carry out the study in the same target region used previously. This proof-of-principle study was designed to characterize the SNAP25 interactome in this series of samples, determine if there was preliminary evidence for a difference between schizophrenia and control samples, and then undertake an initial exploration of the amounts and co-localization of proteins showing differences between schizophrenia and control samples.

EXPERIMENTAL PROCEDURES

Human brain samples

Post-mortem brain samples of the ventromedial caudate (VMC) (Mai et al., 1997; Barakauskas et al., 2010) from 15 subjects with schizophrenia (SCZ) and 13 non-psychiatric

comparison subjects (NPC) were obtained from the Macedonian/New York State Psychiatric Institute Brain Collection (Table 1). Tissue collection, screening and post-mortem diagnosis are detailed elsewhere (Barakauskas et al., 2010). Informed consent was obtained from family members; tissue collection was approved by the Columbia/New York State Psychiatric Institute IRB.

All SCZ subjects had exposure to multiple antipsychotic agents, described in a chart review. Toxicological analyses for drugs of abuse and psychotropic agents were performed on each case. Caffeine and benzodiazepines (available without prescription in Macedonia) were detected during post-mortem toxicological analyses in both NPC and SCZ subjects. Only two SCZ subjects had detectable levels of antipsychotic medications (clozapine).

Immunoprecipitation of SNAP25 for mass spectroscopy

SNAP25 was immunoprecipitated from solubilized brain homogenates using a monoclonal antibody (SP12) that detects both isoforms (Honer et al., 1997; Barakauskas et al., 2010). Samples were coded to mask investigators to diagnosis and sample characteristics. Protocol details were previously published (Barakauskas et al., 2016), and are summarized briefly here. Human brain tissue homogenates (150 μg of crude protein) were solubilized in 0.1% (v/v) Triton X-100/TBS, pre-cleared with empty beads (beads that were not coupled with SP12) and then incubated with SP12-coupled beads for 10 hours. Specificity of immunoprecipitation was monitored by including samples incubated with empty beads. Immunoprecipitates were washed, beads resuspended in Laemelli sample buffer without reducing agent and then stored at −20 °C.

Sample processing for mass spectrometric analysis

Protein samples in Laemelli sample buffer were heated for 10min at ~95 °C, separated by SDS-PAGE and stained with colloidal Coomassie (Barakauskas et al., 2016). For each sample, the gel lane was divided into four segments, plus the 25-kDa area corresponding to SNAP25. The SNAP25 band was used for previously published isoform quantitation studies (Barakauskas et al., 2016). The remaining gel, limited to the area between 15-kDa and 75-kDa size markers and corresponding to proteins which co-immunoprecipitated with SNAP25, was divided into four segments, each corresponding to a known molecular weight range (Fig. 1). The gel segments were cut into ~1 mm^3 pieces placed into a 96-well plate, one segment per well and subjected to in-gel trypsin digestion (Kinter and Sherman, 2005; Cheng et al., 2012). Extracted peptides were lyophilized and stored at −20 °C. Prior to MS analysis, samples were resuspended in 8.5 μl of 1× MS buffer (1% v/v formic acid, 2% v/v acetonitrile).

MS instrumentation

All analyses were performed on a 4000 QTrap (Applied Biosystems/Sciex, Foster City, CA, USA) coupled to an Agilent 1100 Nano-HPLC (Agilent, SantaClara, CA, USA) using a nano-electrospray ionization interface. Samples were desalted online using a reverse-phase trap column (Agilent, Zorbax, 300SB-C18, 5 μm, 5 × 0.3mm) in solvent A (5% acetonitrile, 0.1% formic acid) then directed onto a reverse-phase analytical column (75 μm × 15 cm, packed in-house with 3-μm diameter Reprosil-Pur C18; Dr. Maisch, Ammerbuch-Entringen,

Germany) coupled to an uncoated fused silica emitter tip (20-μm inner diameter, 10-μm tip; New Objective, Woburn, MA, USA). Chromatographic separation used a 300 nl/min flow rate and a linear gradient of 0–23% solvent B (90% acetonitrile, 0.1% formic acid) over 23 min, 23–39% solvent B (over 9 min), and 39% to 80% solvent B (over 4 min).

MS/MS acquisition and protein identification

MS/MS data were collected using a 400–1600 *m/z* Enhanced MS scan followed by an Enhanced Resolution scan to select the top five +2 and +3 ions for collision-induced dissociation and a final enhanced product ion (EPI) MS scan. *M/z* values corresponding to non-specific or contaminating proteins (as determined from control IP conditions) were excluded from EPI scans. Raw mass spectral data were analyzed using Mascot (ver.2.2.2; Matrix Science, Boston, MA, USA) searching against the European Bioinformatics Institute human International Protein Index (IPI) database. Searches were performed with carbamidomethylation of cysteine as a fixed modification, one missed cleavage and a peptide mass tolerance of 0.5 Da. Variable modification search parameters included: oxidation of methionine, deamidation (asparagine, glutamine) and phosphorylation (serine, threonine, tyrosine).

Screening identification of SNAP25 protein interactions in human VMC

Raw spectra from analysis of the gel lane of each sample (Fig. 1) were concatenated and searched against the Ensemble IPI human database (search parameters as outlined above) using Mascot, for each subject separately. In addition, search results for five samples (from five individual subjects) immunoprecipitated under control IP conditions at 2× scale were also processed. The lists of identified proteins were concatenated for the NPC, SCZ and control samples separately, and each list was processed using in-house software (SpecterWeb ver 1.0) by removing proteins identified using less than two peptides, and then removing those found in less than three samples. Additionally, proteins identified with a mean Mascot score <50 across all samples were excluded from further analysis. Filtered protein lists for NPC and SCZ groups were subtracted from each other to determine which proteins were identified in both groups, and which were identified in only one group. Non-specific or contaminating proteins defined as proteins present in one or more control IPs, as well as keratin, were omitted.

Immunoprecipitation for detailed analysis of SNAP25-ARF1 interaction

Immunoprecipitation (IP) of target proteins and their interactive partners was performed using sheep antimouse IgG-coated (for mouse monoclonal primary antibodies) or protein G-coated (for rabbit polyclonal primary antibodies) magnetic Dynabeads (Thermo Fisher Scientific, Waltham, MA, USA), as previously described (Ramos-Miguel et al., 2015a). Briefly, beads were incubated (2 h at room temperature) in the absence (negative control) or presence of primary antibodies (see Appendix Table S1) against SNAP25 (clone SP12), synataxin-1 (clone SP7), or ARF1 (clone ARFS 1A9/5, or rabbit polyclonal) (10 μg of antibody per mg of beads), and diluted in TBS supplemented with 0.1% Triton X-100. Antibody-bead conjugates were blocked for 1 h in TBS supplemented with 3% bovine serum albumin (BSA) and 0.1% Triton X-100. Before IP reactions, human ventromedial caudate (VMC) homogenates from three representative schizophrenia cases were solubilized

in lysis buffer (TBS supplemented with 1 mM ethylenediaminete-traacetic acid (EDTA), 1% protease inhibitor cocktail, and 0.5% Triton X-100), and tissue debris were removed by centrifugation at 16,000*g* for 30 min at 4 °C. Supernatants were precleared with unconjugated magnetic beads for 1 h at 4 °C. Brain samples (0.75 mg protein) were then combined with 0.15 mg of antibody-bead conjugates, and IP reactions were allowed overnight at 4 °C. Finally, IP products were eluted in loading buffer (50 mM Tris, pH 6.8, 10% glycerol, 2% SDS, 100 mM β-mercaptoethanol, 0.01% bromophenol blue) and boiled for 5 min before immunoblotting assays.

Subcellular fractionation and purification of synaptosomes

The synaptosome-enriched fraction, and other subcellular compartments were obtained from human cortical samples (inferior temporal gyrus as VMC samples were limited) as previously described (Ramos-Miguel et al., 2015b). First, brain tissue was carefully homogenized using a motorized glass-Teflon Potter Elvehjem grinder, in a 0.32 M sucrose solution buffered at pH 7.4 with 4 mM hydroxyethylpiperazine ethane sulfonic acid IOD, integrated optical density (HEPES), and supplemented with 1% protease inhibitors. Separation of nuclei (together with tissue debris), cytosol, myelin fragments, synaptosomes and mitochondria was achieved by sequential centrifugation steps followed by resuspension in similar HEPES-buffered solutions with increasing sucrose concentrations (0.8 and 1.2 M) (Gray and Whittaker, 1962; Ramos-Miguel et al., 2015b). The pellets were resuspended in 4 mM HEPES, pH 7.4, divided in appropriate working aliquots, and stored at −80 °C until assayed by immunoblotting and/or immunofluorescence.

Western blotting

We used standard sodium dodecyl sulfate (SDS)-polyacrylamide gel electrophoresis (PAGE), followed by Western immunoblotting (WB), to characterize immunoreactive bands in lysates from human ARF1 transfected and non-transfected 293T cells (see Appendix Table S1), to test IP extractions and subcellular fractionations, as well as to quantify the immunodensity of ARF1 and UQCRC1 in the VMC homogenates from schizophrenia cases and controls. The protocols were extensively detailed previously (Ramos-Miguel et al., 2015b). Briefly, samples were mixed with equal volumes of 2× loading buffer (see above), and boiled for 5 min before loading into 12% minigels (Bio-Rad, Hercules, CA, USA). Prestained molecular markers (Bio-Rad) were loaded in all gels to approximate the molecular weight of the immunoreactive bands. In quantitative studies, all gels also contained a standard sample (pool of all VMC homogenates) in triplicate. After transferring brain proteins to polyvinylidene difluoride (PVDF) membranes (Bio-Rad), nonspecific binding sites were blocked for 1 h at room temperature in TBS containing 5% skim milk and 0.1% Tween-20. Membranes were then incubated with the appropriate primary (overnight at 4 °C; see Appendix Table S1), and horseradish peroxidase-conjugated secondary (1 h at room temperature; 1:5,000 dilution; Jackson ImmunoResearch, West Grove, PA, USA) antibodies, diluted in the same blocking solution. One milliliter of commercial chemiluminescence enhancers (ECL Plus; PerkinElmer, Waltham, MA, USA) was layered on top of the membranes 1 min before imaging the immunoreactive signal in a LAS-3000 reader (Fujifilm, Tokyo, Japan). To control for total protein load, membranes were stripped and reprobed with anti-β-actin antibody. Quantification of the integrated optical density

(IOD) of the immunoreactive bands was done in ImageGauge software, v.4.22 (Fujifilm). The IOD of each of the target immunoreactive bands was first normalized by that of β-actin in the same sample, and then expressed as a percent relative to the mean of the triplicate in-gel standard. Each sample was assayed in three or more different gels, and the mean across these values was taken as a final estimate.

Immunofluorescence and confocal microscopy

To investigate the spatial colocalization of SNAP25 and ARF1 in human presynaptic terminals, synaptosomal extractions were examined by confocal microscopy following double immunolabeling with antibodies against these molecules, essentially as described (Millán et al., 2002). In a poly-L-lysine-coated slide, a 2-by-4 grid of approximately 0.25 cm^2 squares was initially drawn using an ImmEdge hydrophobic barrier PAP pen (Vector Laboratories, Burlingame, CA, USA). In each square, 20 μl of synaptosomal fractions (containing 8 μg of total protein) were spotted, and dried for 30 min at 37 °C. Fixation was accomplished by layering 40 μl of 4% paraformaldehyde for 15 min at room temperature. Excess paraformaldehyde was removed with TBS, and samples were immediately blocked for 1 h in TBS supplemented with 3% BSA and 0.1% Triton X-100. Primary antibodies against SNAP25 (clone SP12; 1:1000), ARF1 (polyclonal; 1:500), vesicular GABA transporter (vGAT; 1:500), and/or vesicular glutamate transporter-1 (vGLUT1, 1:500) were diluted in blocking solution (see Appendix Table S1 for antibody details). Forty μl of these solutions was then added to each square, excluding the negative control(s). After overnight incubation at 4 °C, appropriate combinations of Alexa Fluor 488/555/647-conjugated secondary antibodies (Molecular Probes, Eugene, OR, USA), diluted 1:500 in blocking solution, were overlaid and incubated for 1 h at room temperature in the dark. After gentle washes in TBS, slides were dried for 5 min at 37 °C, overlaid with ProLong Gold Antifade mountant (Molecular Probes), and coverslipped. Samples were imaged in a Zeiss confocal microscope (LSM 5 Pascal; Zeiss, Jena, Germany) equipped with a 63×/1.2NA water immersion objective. Colocalization between the fluorescent probes was analyzed in ImageJ v2.0 (NIH, Bethesda, MA, USA), using unbiased built-in algorithms (Costes et al., 2004; Ramos-Miguel et al., 2015c).

Statistical analysis

Proteins identified in the screening MS/MS phase of the study were compared between the schizophrenia and control samples. A Chi-square test was used to estimate the statistical significance of differences between groups in proportions of samples testing positive for each potentially interacting protein. The *P*-value for significance ($P < 0.05$) was adjusted with the Bonferroni correction method. In subsequent quantitative studies, relationships between target protein amounts and age, postmortem interval, storage time and brain pH were analyzed with Pearson's correlation. The distribution of measures was assessed for normality with the Shapiro-Wilk test. Comparisons between groups used *t*-tests. Cohen's *d* was calculated to estimate effect size.

RESULTS

Samples

Schizophrenia (n = 15) and non-psychiatric control (n = 13) ventromedial caudate samples were the same ones as previously reported to have lower levels of SNAP25, and greater SNAP25-syntaxin interactions in schizophrenia. As noted in Table 1, postmortem interval was longer in the control group, and storage time was longer in the schizophrenia group. These measures, and the others noted in Table 1 were examined for associations with the quantitative measures described below. No statistically significant findings were found, so covariates were not used in comparisons between groups.

SNAP25 protein interactions in human VMC

To explore the local SNAP25 interactome, proteins between ~20 and 75 kDa (Fig. 1) co-immunoprecipitating with SNAP25, but excluding the gel region at 25 kDa, were analyzed by MS/MS. Proteins identified fell into three groups (Table 2). Most consistent, and identified in all samples, were the SNARE and related proteins including SNAP25A, syntaxin-1A and −1B, and VAMP2. Two other proteins, VAMP1 and synapsin-1 were identified as interacting with SNAP25 more frequently in schizophrenia samples. In this screening phase, these findings were not statistically significant after correction for multiple comparisons. Nine other proteins comprised this group, including representatives from syntaxin, synaptotagmin, synapsin and syntaxin-binding protein families. Proteins present in mitochondria (although not necessarily exclusive to mitochondria) were also well represented, with 17 proteins identified. These include VCP transitional endoplasmic reticulum ATPase, identified in all samples. The small GTP-binding protein ADP-ribosylation factor 1 (ARF1) was identified in eight schizophrenia samples and no control samples, a difference that was statistically significant after correction for multiple comparisons (P = 0.0004). The third group was comprised of four proteins of mixed origins, with microfibrillar protein 2 (fragment) identified in all samples. Additional information on the immunoprecipitated proteins appears in Table 3, including a comparison with reports of similar studies using human and rodent brain samples.

ARF1 immunoblotting

Additional studies were carried out to assess ARF1 immunoreactive bands, and quantify ARF1 in total homogenate samples. Lysate from a 293T cell line transfected with human ARF1 displayed an immunoreactive band at approximately 18 kDa (lower than the theoretical molecular weight of 20.7 kDa), detected with a polyclonal antibody and two monoclonal antibodies (Fig. 2A). Samples of human and rat brain homogenates displayed immunoreactive bands at approximately 21 kDa (one polyclonal and one monoclonal antibody), and 17 kDa (one polyclonal and two monoclonal antibodies). The polyclonal antibody was directed at the central region of ARF1, the monoclonal antibodies at the C-terminal region. The immunoreactive bands will be referred to subsequently as ARF1–21 and ARF1–17. These antibodies also reacted with other antigens of higher molecular sizes (37–150 kDa), either corresponding to SDS-resistant oligomers, or spurious bands, which were not considered relevant for the present study. As seen in Fig. 2B, the mean value of ARF1–21 in schizophrenia VMC (87.24, standard deviation (SD) 26.25) was lower than

control samples (110.35, SD 28.94), representing a statistically significant difference (−21%, $P = 0.04$, Cohen's $d = 0.84$). In contrast, ARF1–17 immunodensities did not differ across the diagnostic groups (schizophrenia: 120.87, SD 32.72; NPC: 116.36, SD 28.40). Comparing the ARF1–21 immunodensity between schizophrenia and control using ARF1–17 as a covariate, the lower level of ARF1–21 in the schizophrenia samples remained statistically significant ($P = 0.01$).

For comparison with ARF1 (Fig. 2B), the mitochondrial marker UQCRC1 (ubiquinol-cytochrome c reductase core protein 1) was also quantified. The mean value in schizophrenia VMC (94.18, SD 22.10) did not differ from the control value (107.47, SD 17.84). As previously reported (Barakauskas et al., 2010), in schizophrenia these same samples had lower SNAP25, and higher SNAP25-syntaxin interactions than control samples. These two measures were inversely correlated - a low level of SNAP25 was associated with a high SNAP25-syntaxin protein-protein interaction (Table 4). Neither of these measures showed an association with the level of the mitochondrial protein UQCRC1. Lower ARF1–21 was associated with greater SNAP25-syntaxin interaction. Levels of ARF1–17 were positively correlated with ARF1–21, but not with SNAP25 or with the SNAP25-syntaxin interaction. There was a positive association between the mitochondrial protein UQCRC1 and ARF1–21, but no association with ARF1–17.

Characterization of ARF1-SNAP25 interaction

To confirm and further characterize the ARF1-SNAP25 interaction, we co-immunoprecipitated these (and other synaptic) targets from a pool of three schizophrenia VMC homogenates, where this interaction was previously identified in MS/MS experiments. Interestingly, IP assays using anti-SNAP25 and antisyntaxin-1 antibodies revealed that only ARF1–21, but not ARF1–17, precipitated along with the SNARE proteins (Fig. 3A). However, both SNARE proteins were pulled down in ARF1-IP assays, regardless of the anti-ARF1 antibody used. The latter observation indicates that the anti-ARF1 monoclonal antibody may recognize the ARF1–21 epitope only under native conditions, but not following SDS-PAGE. Furthermore, ARF1-IP reactions were highly enriched in other synaptic structural proteins known to play a role in SNARE-mediated exocytosis, such as septin 5 (SEPT5, also called CDCrel-1) (Fig. 3A). This finding may raise the question of whether the ARF1-SNAP25 interaction occurs directly or via intermediate partners such as SEPT5. Of note, the above protein-protein interactions were not the result of whole organelle precipitation during IP assays, as the mitochondrial marker UQCRC1 was not present in either IP reaction (Fig. 3A).

Subcellular fractionation experiments showed that the ARF1-SNAP25 association is anatomically relevant, as both ARF1 species were present in the synaptosomal preparations (Fig. 3B). Of interest, ARF1–21 was relatively enriched in the synaptic compartment compared to the cytosolic fraction. The presence of ARF1 species in the nucleus could not be confirmed, since large amounts of post-mortem tissue debris containing proteins from all compartments precipitate along with the nuclear fraction under the present assay conditions.

The colocalization between ARF1 and SNAP25 within the synaptosomes was further confirmed by confocal microscopy (Fig. 3C). Indeed, the vast majority of ARF1 signal was

detected within SNAP25-positive particles, suggesting that this molecule is mainly expressed in the presynaptic, rather than postsynaptic terminals. Remarkably, in the same synaptosomal preparations, the distribution of ARF1 across the terminal subtypes was also unbalanced. ARF1 expression in vGLUT1-positive (i.e. excitatory) synaptosomes was fivefold greater compared with expression in vGAT-positive (i.e. inhibitory) particles (Fig. 3D, E).

DISCUSSION

In the series of ventromedial caudate schizophrenia samples with lower levels of SNAP25, and greater SNAP25-syntaxin interaction, SNAP25 immunoprecipitation and mass spectrometry demonstrated the expected interactions between SNAP25 and other SNARE-related proteins. Detection of these interactions was somewhat more frequent in schizophrenia compared with control samples, consistent with the previous report of a quantitative increase in SNAP25-syntaxin interaction in these samples (Barakauskas et al., 2010). Associations between SNAP25 and proteins also found in mitochondria were observed. Specifically, the interaction between SNAP25 and the mitochondrial small GTPase ARF1 appeared to be more frequently detected in co-immunoprecipitates from the schizophrenia samples. Independent assessment of ARF1 levels in brain homogenates using immunoblotting showed lower levels in the schizophrenia samples. Fractionation studies and co-localization using confocal microscopy supported the immunoprecipitation evidence for SNAP25-ARF1 protein-protein interaction.

The SNARE complex was initially characterized with immunoaffinity purification techniques (Söllner et al., 1993a,b). Subsequent studies expanded characterization of SNARE interacting and modulating proteins, and demonstration of the importance of the SNARE complex in neurotransmission suggested SNARE and interacting proteins as targets for investigation in schizophrenia (Katrancha and Koleske, 2015). As well, converging evidence from screening studies of gene expression using microarray techniques indicated the importance of changes in the presynaptic compartment to the pathophysiology of the illness (Mirnics et al., 2000). Meta analysis of presynaptic proteins in schizophrenia provides evidence for lower levels of synaptophysin (Osimo et al., 2018), a protein present in most if not all synapses, but enriched in glutamatergic synapses (Grønborg et al., 2010). For SNARE and SNARE-interacting proteins, the findings related to protein levels in schizophrenia are more variable (Egbujo et al., 2016; Osimo et al., 2018). This is not surprising, as even in age-related cognitive impairment and frank Alzheimer’s disease, presynaptic protein changes are heterogeneous, showing relationships to extent of pathology, acting as part of neural reserve, and having variable associations depending on brain region (Minger et al., 2001; Honer, 2003; Boyle et al., 2013; Ramos-Miguel et al., 2017).

SNARE protein-protein interactions may be more informative than protein levels, as seen in studies of schizophrenia and of age-related cognitive impairment (Honer et al., 2002; Barakauskas et al., 2010; Ramos-Miguel et al., 2015a). An animal model with a dominant isoleucine-to-threonine mutation in the SNAP25 protein has increased interaction between SNAP25 and syntaxin, and demonstrates phenotypic features consistent with some aspects of schizophrenia (Jeans et al., 2007; Oliver and Davies, 2009; Oliver et al., 2012).

Interactions between SNARE and related proteins may also be increased, including complexes containing syntaxin-binding protein-1 and complexin-1 (Ramos-Miguel et al., 2015a). As expected, the immunoprecipitation and mass spectrometry results from the present study identify multiple interacting proteins, also reported in studies of human or rodent SNAP25 interactomes (Gorini et al., 2010; Brinkmalm et al., 2014). Most of these proteins, and their interactions with SNAP25, are not yet studied in schizophrenia samples, and could be targets for future investigation.

As well as interactions with proteins directly involved in neurotransmission, constituents of the mitochondrial proteome were also immunoprecipitated along with SNAP25. Mitochondrial proteins are identified as being dysregulated in proteomic studies of depression and schizophrenia (Pennington et al., 2008; Saia-Cereda and Martins-de-Souza, 2017). Studies have not yet focussed on synaptic mitochondria specifically; the proteome of mitochondria in the presynaptic compartment may differ quantitatively from non-synaptic mitochondria (Stauch et al., 2014; Völgyi et al., 2015; Villa et al., 2017). The interpretation of the SNAP25 co-immunoprecipitation findings is complex. Proteins enriched in presynaptic terminal organelles such as vesicles are also present in mitochondria (Burré and Volknandt, 2007; Barth and Volknandt, 2011; Völgyi et al., 2015). Mitochondrial fragments could co-immunoprecipitate, providing the possibility of detection due to proximity. Studies using electron microscopy sometimes demonstrate mitochondria attached to active zone membranes (Laßek et al., 2015). Direct interactions between proteins usually categorized as synaptic, and those assigned to mitochondria may occur, as well as detection of apparent interactions due to proximity of localization.

The small GTPase ARF1 has multiple cellular functions and distribution (Bottanelli et al., 2017), and was recently reported to be a constituent of mitochondria (Ackema et al., 2014; Rabouille, 2014; Spang, 2015). Detection of ARF1 in schizophrenia but not control SNAP25 immunoprecipitates was followed up by measuring ARF1 levels in homogenates. ARF1 was detected in all samples, and ARF1–21 was found by immunoblotting to be 21% lower in schizophrenia. Another study reported higher ARF1 levels in depression with psychosis compared with depression free of psychosis, however samples from depression as a whole did not differ from control samples (Martins-de-Souza et al., 2012). The discordance between the lower level and the possibly greater interaction in schizophrenia is similar to the effect of this illness on SNAP25 and syntaxin levels (lower) and the interaction between these proteins (greater) (Barakauskas et al., 2010). Lower ARF1–21 levels were statistically associated with greater SNAP25-syntaxin interaction. A novel finding was the presence of at least two ARF1 immunoreactive protein bands co-occurring in human brain tissue, as resolved by SDS-PAGE followed by immunoblotting. ARF1 is subject to post-translational modification through myristoylation, and also demonstrates dimerization, properties that can alter the distribution of immunoreactive bands following electrophoresis (Beck et al., 2008). Whether ARF1–21 and 17 represent different variants of the same gene, or are the result of post-translational modifications was beyond the scope of the present study. However, taking into account their differential binding profiles (only ARF1–21 appeared to interact with the SNARE proteins), as well as their subcellular distributions (ARF1–21 mainly in synaptic fractions and ARF1–17 being more abundant in the cytosol), it is tempting to speculate that these ARF1 species might be involved in different cellular processes in the brain.

Interestingly, the levels of ARF1–21 were correlated with levels of the mitochondrial protein UQCRC1, while those of ARF1–17 were not. ARF1 immunoprecipitates contained the protein SEPT5, a GTP-binding protein reported to be enriched in docked synaptic vesicle fractions (Boyken et al., 2013). SEPT5 levels were reported to be elevated in prefrontal cortex in bipolar disorder and schizophrenia (Pennington et al., 2008), and relatively lower in neurodegenerative disease (Marttinen et al., 2015). The present immunocytochemical studies showed more ARF1 in glutamatergic human synaptosomes than in GABAergic, consistent with findings in rodents (Grønborg et al., 2010; Boyken et al., 2013).

Outside of the SNARE-associated and mitochondrial proteins, several of the proteins with preliminary evidence (Table 2) for being present in SNAP25 immunoprecipitates are of interest for neuropsychiatric illness. As examples:

MAP1B interacts with the mGluR4 presynaptic receptor (Moritz et al., 2009).

FHL1 (four and a half LIM domains 1 isoform 5) is associated with X-linked myopathies (Shathasivam et al., 2010).

VCP transitional endoplasmic reticulum ATPase is associated with Paget's disease, amyotrophic lateral sclerosis, has mutations in some types of fronto-temporal dementia and interacts with mitochondrial proteins (Zhang et al., 2017).

The primary limitation of the present study is the small sample size. The results must be considered preliminary, and hypothesis-generating, requiring replication in an independent series of samples. None the less, the observation of a possible connection between abnormalities of presynaptic protein-protein interactions, and synaptic mitochondria supports a new research strategy of including studies of mitochondria as part of the evaluation of presynaptic terminals in schizophrenia. More detailed studies of the individual proteins identified here are needed to determine the extent to which the protein-protein interactions are specific (Li et al., 2012). While multiple negative controls were used, and additional work with independent assays was carried out for ARF1 and SNAP25, more definitive studies are needed for the full range of putative targets identified. These could include electron microscopy, to help discern the likelihood of adhesion of mitochondria to the presynaptic membrane, leading to immunoprecipitation by proximity, rather than a specific protein-protein interaction (Boyken et al., 2013).

CONCLUSIONS

The present findings support previous studies demonstrating the importance of the SNAP25 interactome in schizophrenia and in neurodegenerative disease (Katrancha and Koleske, 2015; Ramos-Miguel et al., 2015a, 2018). Expanding investigation of the interactome beyond SNARE proteins, to include mitochondrial proteins and function, offers a new strategy to characterize the origins and mechanism of presynaptic dysfunction in schizophrenia.

Supplementary Material

Refer to Web version on PubMed Central for supplementary material.

ACKNOWLEDGMENTS

The study was supported by the Canadian Institutes of Health Research (MT-14037, MOP-81112) and the National Institute of Mental Health (MH60877, MH64168, MH62185, MH45212, MH64673), National Alliance for Research on Schizophrenia and Depression, and the Lieber Center for Schizophrenia Research. We thank Hong-Ying Li and Jenny Yang for their skillful assistance.

Abbreviations:

ARF1	ADP-ribosylation factor 1
ARF1–17	ARF1 17 kiloDaltons
ARF1–21	ARF1 21 kiloDaltons
BSA	bovine serum albumin
DSM-IV	Diagnostic and Statistical Manual for Mental Disorders, 4th Edition
EPI	enhanced product ion
FHL1	four and a half LIM domains 1 isoform 5
GABA	gamma-aminobutyric acid
IP	immunoprecipitation
IPI	International Protein Index
MAG	myelin-associated glycoprotein
MAP1B	microtubule-associated protein 1B
MS	mass spectroscopy
NPC	non-psychiatric comparison
PAGE	polyacrylamide gel electrophoresis
PMI	postmortem interval
PVDF	polyvinylidene difluoride
SCZ	schizophrenia
SDS	sodium dodecyl sulfate
SEPT5	septin 5
SNAP25 (or S25)	synaptosome-associated protein 25

SNARE	soluble N-ethylmaleimide-sensitive factor attachment protein receptor
TBS	Tris-buffered saline
UQCRC1	ubiquinol-cytochrome c reductase core protein 1
VAMP	vesicle-associated membrane protein
VCP	valosin-containing protein transitional endoplasmic reticulum ATPase
vGAT	vesicular GABA transporter
vGLUT1	vesicular glutamate transporter-1
VMC	ventromedial caudate
WB	Western immunoblotting

REFERENCES

Abi-Dargham A, van de Giessen E, Slifstein M, Kegeles LS, Laruelle M (2009) Baseline and amphetamine-stimulated dopamine activity are related in drug-naïve schizophrenic subjects. Biol Psychiatry 65:1091–1093. [PubMed: 19167701]

Ackema KB, Hench J, Böckler S, Wang SC, Sauder U, Mergentaler H, Westermann B, Bard F, Frank S, Spang A (2014) The small GTPase Arf1 modulates mitochondrial morphology and function. EMBO J 33:2659–2675. [PubMed: 25190516]

Barakauskas VE, Beasley CL, Barr AM, Ypsilanti AR, Li H-Y, Thornton AE, Wong H, Rosokilja G, Mann JJ, Mancevski B, Jakovski Z, Davceva N, Ilievski B, Dwork AJ, Falkai P, Honer WG (2010) A novel mechanism and treatment target for presynaptic abnormalities in specific striatal regions in schizophrenia. Neuropsychopharmacology 35:1226–1238. [PubMed: 20072114]

Barakauskas VE, Moradian A, Barr AM, Beasley CL, Rosoklija G, Mann JJ, Ilievski B, Stankov A, Dwork AJ, Falkai P, Morin GB, Honer WG (2016) Quantitative mass spectrometry reveals changes in SNAP-25 isoforms in schizophrenia. Schizophr Res 177:44–51. [PubMed: 26971072]

Barth J, Volknandt W (2011) Proteomic investigations of the synaptic vesicle interactome. Expert Rev Proteomics 8:211–220. [PubMed: 21501014]

Beck R, Sun Z, Adolf F, Rutz C, Bassler J, Wild K, Sinning I, Hurt E, Brugger B, Bethune J, Wieland F (2008) Membrane curvature induced by ARF1-GTP is essential for vesicle formation. Proc Nat Acad Sci USA 105:11731–11736. [PubMed: 18689681]

Bottanelli F, Kilian N, Ernst AM, Rivera-Molina F, Schroeder LK, Kromann EB, Lessard MD, Erdmann RS, Schepartz A, Baddeley D, Bewersdorf J, Toomre D, Rothman JE (2017) A novel physiological role for ARF1 in the formation of bidirectional tubules from the Golgi Glick BS, ed. Mol Biol Cell 28:1676–1687. [PubMed: 28428254]

Boyken J, Grønborg M, Urlaub H, Jahn R (2013) Molecular profiling of synaptic vesicle docking sites reveals novel proteins but few differences between glutamatergic and GABAergic synapses. Neuron 78:285–297. [PubMed: 23622064]

Boyle PA, Yu L, Honer WG, Schneider JA (2013) Much of late life cognitive decline is not due to common neurodegenerative pathologies. Ann Neurol 74:478–489. [PubMed: 23798485]

Brinkmalm A, Brinkmalm G, Honer WG, Moreno JA, Jakobsson J, Mallucci GR, Zetterberg H, Blennow K, Ohrfelt A (2014) Targeting synaptic pathology with a novel affinity mass spectrometry approach. Mol Cell Proteomics 13:2584–2592. [PubMed: 24973420]

Burré J, Volknandt W (2007) The synaptic vesicle proteome. J Neurochem 101:1448–1462. [PubMed: 17355250]

Cheng S-WG, Kuzyk MA, Moradian A, Ichu T-A, Chang VC-D, Tien JF, Vollett SE, Griffith M, Marra MA, Morin GB (2012) Interaction of cyclin-dependent kinase 12/CrkRS with cyclin K1 is required for the phosphorylation of the C-terminal domain of RNA polymerase II. Mol Cell Biol 32:4691–4704. [PubMed: 22988298]

Costes SV, Daelemans D, Cho EH, Dobbin Z, Pavlakis G, Lockett S (2004) Automatic and quantitative measurement of proteinprotein colocalization in live cells. Biophys J 86:3993–4003. [PubMed: 15189895]

Dean B, Thomas N, Lai C-Y, Chen WJ, Scarr E (2015) Changes in cholinergic and glutamatergic markers in the striatum from a subset of subjects with schizophrenia. Schizophr Res 169:83–88. [PubMed: 26545297]

Demjaha A, Egerton A, Murray RM, Kapur S, Howes OD, Stone JM, McGuire PK (2014) Antipsychotic treatment resistance in schizophrenia associated with elevated glutamate levels but normal dopamine function. Biol Psychiatry 75:e11–e13. [PubMed: 23890739]

Demjaha A, Murray RM, McGuire PK, Kapur S, Howes OD (2012) Dopamine synthesis capacity in patients with treatment-resistant schizophrenia. Am J Psychiatry 169:1203–1210. [PubMed: 23034655]

Egbujo CN, Sinclair D, Hahn C-G (2016) Dysregulations of synaptic vesicle trafficking in schizophrenia. Curr Psychiatry Rep 18:77. [PubMed: 27371030]

Gorini G, Ponomareva O, Shores KS, Person MD, Harris RA, Mayfield RD (2010) Dynamin-1 co-associates with native mouse brain BKCa channels: proteomics analysis of synaptic protein complexes. FEBS Lett 584:845–851. [PubMed: 20114047]

Gray EG, Whittaker VP (1962) The isolation of nerve endings from brain: an electron-microscopic study of cell fragments derived by homogenization and centrifugation. J Anat 96:79–88. [PubMed: 13901297]

Grønborg M, Pavlos NJ, Brunk I, Chua JJE, Münster-Wandowski A, Jahn R (2010) Quantitative comparison of glutamatergic and GABAergic synaptic vesicles unveils selectivity for few proteins including MAL2, a novel synaptic vesicle protein. J Neurosci 30:2–12. [PubMed: 20053882]

Honer WG, Hu L, Davies P (1993) Human synaptic proteins with a heterogeneous distribution in cerebellum and visual cortex. Brain Res 609:9–20. [PubMed: 7685234]

Honer WG (2003) Pathology of presynaptic proteins in Alzheimer's disease: more than simple loss of terminals. NBA 24:1047–1062.

Honer WG, Falkai P, Bayer TA, Xie J, Hu L, Li H-Y, Arango V, Mann JJ, Dwork AJ, Trimble WS (2002) Abnormalities of SNARE mechanism proteins in anterior frontal cortex in severe mental illness. Cereb Cortex 12:349–356. [PubMed: 11884350]

Honer WG, Falkai P, Young C, Wang T, Xie J, Bonner J, Hu L, Boulianne GL, Luo Z, Trimble WS (1997) Cingulate cortex synaptic terminal proteins and neural cell adhesion molecule in schizophrenia. Neuroscience 78:99–110. [PubMed: 9135092]

Howes OD, Montgomery AJ, Asselin M-C, Murray RM, Valli I, Tabraham P, Bramon-Bosch E, Valmaggia L, Johns L, Broome M, McGuire PK, Grasby PM (2009) Elevated striatal dopamine function linked to prodromal signs of schizophrenia. Arch Gen Psychiatry 66:13–20. [PubMed: 19124684]

Jeans AF, Oliver PL, Johnson R, Capogna M, Vikman J, Molnár Z, Babbs A, Partridge CJ, Salehi A, Bengtsson M, Eliasson L, Rorsman P, Davies KE (2007) A dominant mutation in Snap25 causes impaired vesicle trafficking, sensorimotor gating, and ataxia in the blind-drunk mouse. Proc Natl Acad Sci USA 104:2431–2436. [PubMed: 17283335]

Katrancha SM, Koleske AJ (2015) SNARE complex dysfunction: A unifying hypothesis for schizophrenia. Biol Psychiatry 78:356–358. [PubMed: 26296424]

Kegeles LS, Abi-Dargham A, Frankle WG, Gil R, Cooper TB, Slifstein M, Hwang D-R, Huang Y, Haber SN, Laruelle M (2010) Increased synaptic dopamine function in associative regions of the striatum in schizophrenia. Arch Gen Psychiatry 67:231–239. [PubMed: 20194823]

Kinter M, Sherman NE (2005) Protein sequencing and identification using tandem mass spectrometry. Hoboken, NJ, USA: John Wiley & Sons Inc.

Laßek M, Weingarten J, Volknandt W (2015) The synaptic proteome. Cell Tissue Res 359:255–265. [PubMed: 25038742]

Li KW, Chen N, Klemmer P, Koopmans F, Karupothula R, Smit AB (2012) Identifying true protein complex constituents in interaction proteomics: the example of the DMXL2 protein complex Lubec G, ed. Proteomics 12:2428–2432. [PubMed: 22707207]

Mai JK, Assheuer J, Paxinos G (1997) Atlas of the human brain. San Diego: Academic Press.

Martins-de-Souza D, Cassoli JS, Nascimento JM, Hensley K (2015) The protein interactome of collapsin response mediator protein-2 (CRMP2/DPYSL2) reveals novel partner proteins in brain tissue. Martins-de-Souza D, ed. Prot Clin Appl 9:817–831.

Martins-de-Souza D, Guest PC, Harris LW, Vanattou-Saifoudine N, Webster MJ, Rahmoune H, Bahn S (2012) Identification of proteomic signatures associated with depression and psychotic depression in post-mortem brains from major depression patients. Transl Psychiatry 2:e87. [PubMed: 22832852]

Marttinen M, Kurkinen KM, Soininen H, Haapasalo A, Hiltunen M (2015) Synaptic dysfunction and septin protein family members in neurodegenerative diseases. Mol Neurodegener 10:16. [PubMed: 25888325]

Millán C, Luján R, Shigemoto R, Sanchez-Prieto J (2002) Subtype-specific expression of group III metabotropic glutamate receptors and Ca2+ channels in single nerve terminals. J Biol Chem 277:47796–47803. [PubMed: 12376542]

Minger SL, Honer WG, Esiri MM, McDonald B, Keene J, Nicoll JA, Carter J, Hope T, Francis PT (2001) Synaptic pathology in prefrontal cortex is present only with severe dementia in Alzheimer disease. J Neuropathol Exp Neurol 60:929–936. [PubMed: 11589423]

Mirnics K, Middleton FA, Marquez A, Lewis DA, Levitt P (2000) Molecular characterization of schizophrenia viewed by microarray analysis of gene expression in prefrontal cortex. Neuron 28:53–67. [PubMed: 11086983]

Morciano M, Beckhaus T, Karas M, Zimmermann H, Volknandt W (2009) The proteome of the presynaptic active zone: from docked synaptic vesicles to adhesion molecules and maxi-channels. J Neurochem 108:662–675. [PubMed: 19187093]

Moritz A, Scheschonka A, Beckhaus T, Karas M, Betz H (2009) Metabotropic glutamate receptor 4 interacts with microtubule-associated protein 1B. Biochem Biophys Res Commun 390:82–86. [PubMed: 19781524]

Oliver PL, Davies KE (2009) Interaction between environmental and genetic factors modulates schizophrenic endophenotypes in the Snap-25 mouse mutant blind-drunk. Hum Mol Genet 18:4576–4589. [PubMed: 19729413]

Oliver PL, Sobczyk MV, Maywood ES, Edwards B, Lee S, Livieratos A, Oster H, Butler R, Godinho SIH, Wulff K, Peirson SN, Fisher SP, Chesham JE, Smith JW, Hastings MH, Davies KE, Foster RG (2012) Disrupted circadian rhythms in a mouse model of schizophrenia. Curr Biol 22:314–319. [PubMed: 22264613]

Osimo EF, Beck K, Reis Marques T, Howes OD (2018) Synaptic loss in schizophrenia: a meta-analysis and systematic review of synaptic protein and mRNA measures. Mol Psychiatry 42:139.

Pennington K, Beasley CL, Dicker P, Fagan A, English J, Pariante CM, Wait R, Dunn MJ, Cotter DR (2008) Prominent synaptic and metabolic abnormalities revealed by proteomic analysis of the dorsolateral prefrontal cortex in schizophrenia and bipolar disorder. Mol Psychiatry 13:1102–1117. [PubMed: 17938637]

Perez-Costas E, Melendez-Ferro M, Roberts RC (2010) Basal ganglia pathology in schizophrenia: dopamine connections and anomalies. J Neurochem 113:287–302. [PubMed: 20089137]

Rabouille C (2014) Old dog, new tricks: Arf1 required for mitochondria homeostasis. EMBO J 33:2604–2605. [PubMed: 25230932]

Ramos-Miguel A, Beasley CL, Dwork AJ, Mann JJ, Rosoklija G, Barr AM, Honer WG (2015a) Increased SNARE protein-protein interactions in orbitofrontal and anterior cingulate cortices in schizophrenia. Biol Psychiatry 78:361–373. [PubMed: 25662103]

Ramos-Miguel A, Hercher C, Beasley CL, Barr AM, Bayer TA, Falkai P, Leurgans SE, Schneider JA, Bennett DA, Honer WG (2015b) Loss of Munc18–1 long splice variant in GABAergic terminals is associated with cognitive decline and increased risk of dementia in a community sample. Mol Neurodegener 10:65. [PubMed: 26628003]

Ramos-Miguel A, Honer WG, Boyda HN, Sawada K, Beasley CL, Procyshyn RM, Barr AM (2015c) Exercise prevents downregulation of hippocampal presynaptic proteins following olanzapine-elicited metabolic dysregulation in rats: Distinct roles of inhibitory and excitatory terminals. Neuroscience 301:298–311. [PubMed: 26086543]

Ramos-Miguel A, Jones AA, Sawada K, Barr AM, Bayer TA, Falkai P, Leurgans SE, Schneider JA, Bennett DA, Honer WG (2018) Frontotemporal dysregulation of the SNARE protein interactome is associated with faster cognitive decline in old age. Neurobiol Dis 114:31–44. [PubMed: 29496544]

Ramos-Miguel A, Sawada K, Jones AA, Thornton AE, Barr AM, Leurgans SE, Schneider JA, Bennett DA, Honer WG (2017) Presynaptic proteins complexin-I and complexin-II differentially influence cognitive function in early and late stages of Alzheimer's disease. Acta Neuropathol 133:395–407. [PubMed: 27866231]

Roberts RC (2017) Postmortem studies on mitochondria in schizophrenia. Schizophr Res 187:17–25. [PubMed: 28189530]

Roberts RC, Roche JK, Conley RR (2005) Synaptic differences in the postmortem striatum of subjects with schizophrenia: a stereological ultrastructural analysis. Synapse 56:185–197. [PubMed: 15803499]

Roberts RC, Roche JK, Conley RR (2008) Differential synaptic changes in the striatum of subjects with undifferentiated versus paranoid schizophrenia. Synapse 62:616–627. [PubMed: 18509852]

Saia-Cereda VM, Martins-de-Souza D(2017) The energy metabolism dysfunction in psychiatric disorders postmortem brains: Focus on proteomic evidence. Front Neurosci 11:493. [PubMed: 28936160]

Shathasivam T, Kislinger T, Gramolini AO (2010) Genes, proteins and complexes: the multifaceted nature of FHL family proteins in diverse tissues. J Cell Mol Med 14:2702–2720. [PubMed: 20874719]

Söllner T, Bennett MK, Whiteheart SW, Scheller RH, Rothman JE (1993a) A protein assembly-disassembly pathway in vitro that may correspond to sequential steps of synaptic vesicle docking, activation, and fusion. Cell 75:409–418. [PubMed: 8221884]

Söllner T, Whiteheart SW, Brunner M, Erdjument-Bromage H, Geromanos S, Tempst P, Rothman JE (1993b) SNAP receptors implicated in vesicle targeting and fusion. Nature 362:318–324. [PubMed: 8455717]

Spang A (2015) A small GTPase involved in mitochondrial morphology and function. Biochem Soc Trans 43:108–110. [PubMed: 25619254]

Stauch KL, Purnell PR, Fox HS (2014) Quantitative proteomics of synaptic and nonsynaptic mitochondria: insights for synaptic mitochondrial vulnerability. J Proteome Res 13:2620–2636. [PubMed: 24708184]

Villa RF, Ferrari F, Bagini L, Gorini A, Brunello N, Tascedda F (2017) Mitochondrial energy metabolism of rat hippocampus after treatment with the antidepressants desipramine and fluoxetine. Neuropharmacology 121:30–38. [PubMed: 28431972]

Völgyi K, Gulyássy P, Háden K, Kis V, Badics K, Kékesi KA, Simor A, Györffy B, Tóth EA, Lubec G, Juhasz G, Dobolyi A (2015) Synaptic mitochondria: a brain mitochondria cluster with a specific proteome. J Proteomics 120:142–157. [PubMed: 25782751]

Wilhelm BG, Mandad S, Truckenbrodt S, Kröhnert K, Schäfer C, Rammner B, Koo SJ, Claßen GA, Krauss M, Haucke V, Urlaub H, Rizzoli SO (2014) Composition of isolated synaptic boutons reveals the amounts of vesicle trafficking proteins. Science 344:1023–1028. [PubMed: 24876496]

Zhang T, Mishra P, Hay BA, Chan D, Guo M (2017) Valosin-containing protein (VCP/p97) inhibitors relieve Mitofusin-dependent mitochondrial defects due to VCP disease mutants. Elife 6.

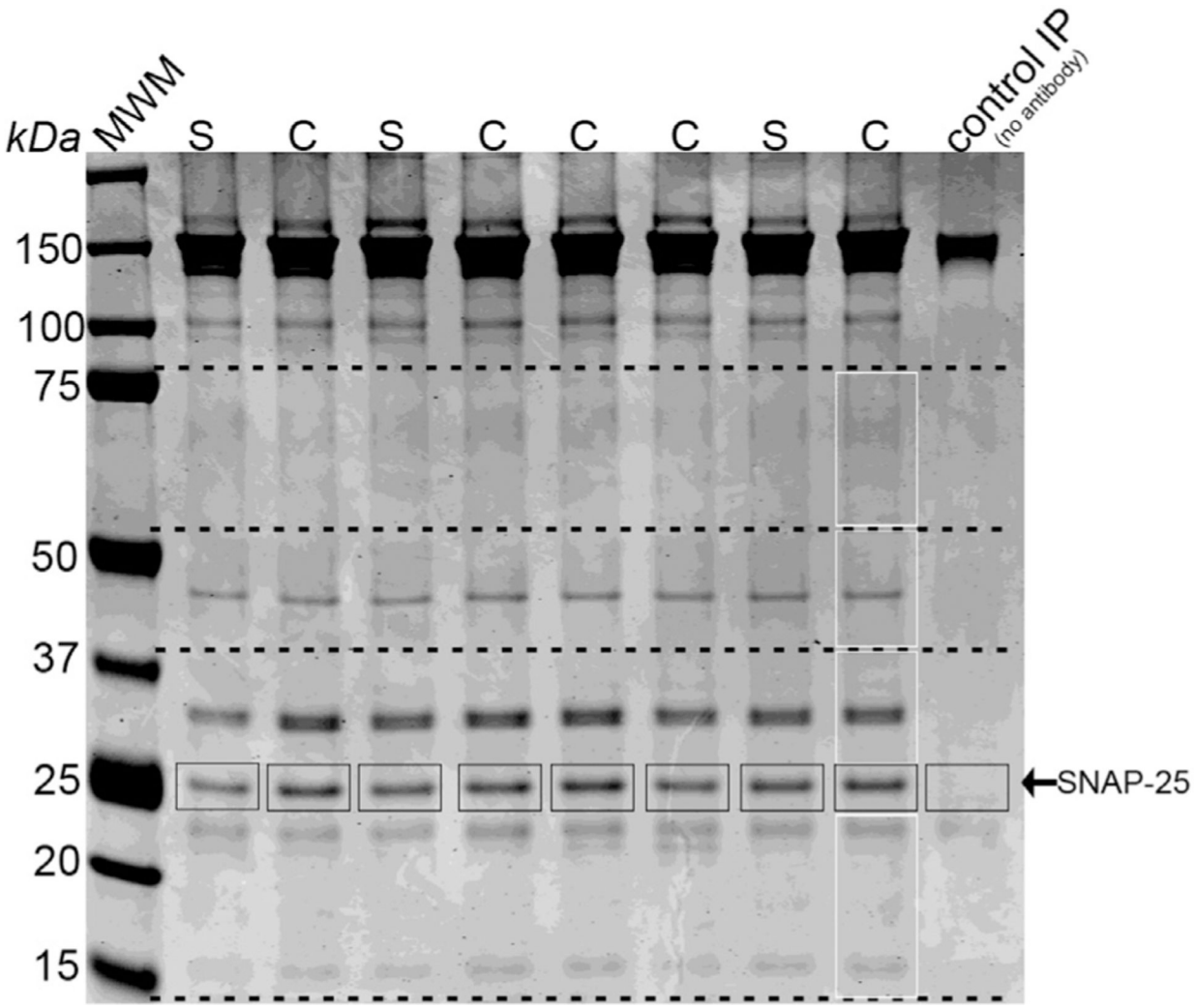

Fig. 1.

Gel sampling for MS/MS analysis. Example of the landmarks used to cut gel lanes of Coomassie-stained SNAP25 immunoprecipiates. The band containing SNAP25 was omitted in the present analysis (outlined in black). For MS/MS analysis, the remaining gel was assayed between the 75-kDa and 15-kDa markers (dashed lines) and each sample lane was divided into four pieces (white boxes and dashed lines) for processing, digestion and MS/MS analysis. Raw spectra from the four gel pieces were combined then searched using Mascot to identify proteins that co-immunoprecipitate with SNAP25. An example of a control immunoprecipitation is also given, and illustrates non-specific bands, and the absence of SNAP25 under control conditions. Higher molecular weight bands (>100 kDa) consist of antibody and material from the beads. *Abbreviations*: IP, immunoprecipitation; S, schizophrenia; C, non-psychiatric comparison subject; MWM, molecular weight marker.

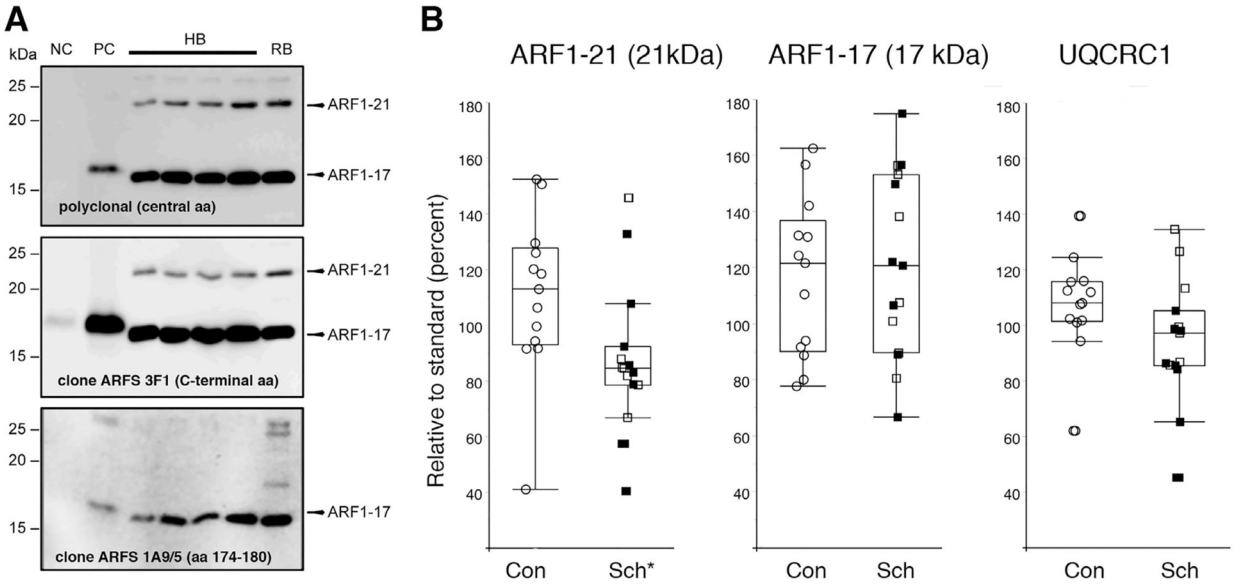

Fig. 2.

Characterization of ARF1 imunoreactivity, and quantification of immunoreactivity in control and schizophrenia ventromedial caudate samples. (A) Immunodetection of ARF1 in non-transfected 293T cells (negative control NC) and human ARF1 transfected cells (positive control PC), followed by 4 human brain homogenate samples (HB) and rat brain homogenate (RB). A polyclonal (upper panel) and two monoclonal antibodies were used. Molecular masses (in kDa) of prestained standards are shown on the left. (B) Boxplots show ARF1–21, ARF1–17 and the mitochondrial protein UQCRC1 normalized to beta-actin, and expressed as a percentage relative to the mean of the triplicate in-gel standards. Filled boxes in the schizophrenia plots represent samples that showed SNAP25– ARF1 interaction in the mass spectroscopy study. *Difference between control (Con) and schizophrenia (Sch) samples, $P < 0.05$.

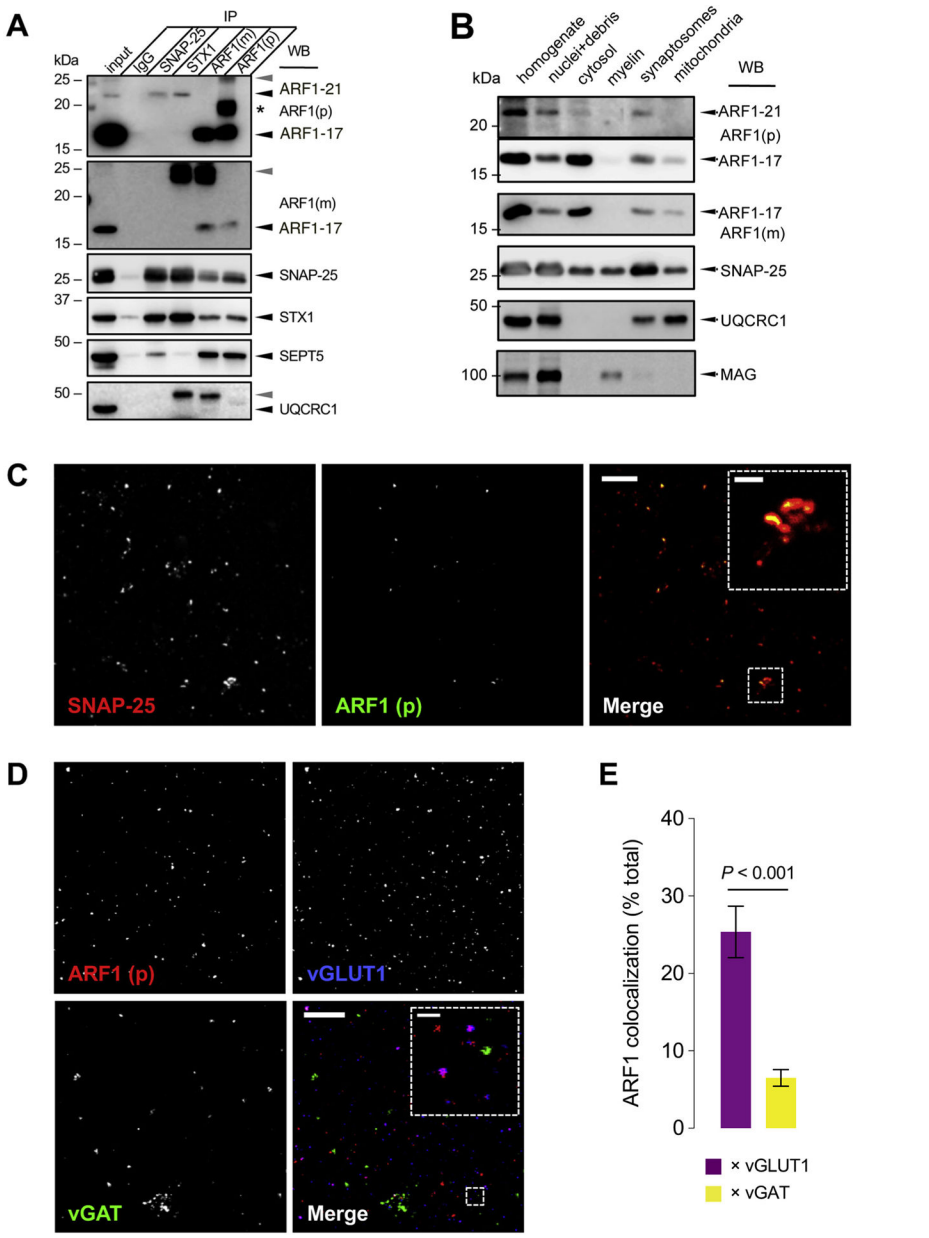

Fig. 3.

Characterization of SNAP25-ARF1 interaction. (A) Co-immunoprecipitation (IP) assays of SNAP25, syntaxin-1 (STX1), and ARF1 (monoclonal and polyclonal antibodies) confirmed SNAP25 interaction with ARF1–21 but not ARF-17 in VMC homogenates from three representative subjects with schizophrenia. Additionally, ARF1 appears to interact with other SNARE proteins (STX1) and partners (septin 5; SEPT5). The SNAP25-ARF1 interaction does not involve full mitochondria pull-down, as the mitochondrial marker UQCRC1 (ubiquinol-cytochrome c reductase core protein 1; a core component of the Complex III) did not precipitate along with the SNAREs or ARF1. Black arrowheads indicate specific protein targets whereas gray arrowheads indicate bands matching the immunoglobulins used in IP assays. The band adjacent to the asterisk was not observed

consistently and may be an artifact. (B) Sequential fractionation of subcellular compartments in postmortem human brain samples (three different subjects were tested with similar results) revealed a relative enrichment of ARF1–21 in the synaptosomal extractions, compared to ARF1–17. The ARF1–21 and 17 images for the polyclonal antibody were chosen from the same blot at different exposure times to maximize visualization. Membranes were also immunoblotted for UQCRC1 and myelin-associated glycoprotein (MAG) as markers of the myelin and mitochondrial extractions, respectively. (A, B) Molecular masses (in kDa) of prestained standards are shown on the left. (C) Confocal microphotographs of human synaptosomal extractions co-immunolabeled with SNAP25 (clone SP12; red) and ARF1 (polyclonal; green) antibodies, showing the positive colocalization of both molecules at synaptic terminals. (D) Microphotographs obtained as above following triple co-immunostaining with antibodies against ARF1 (polyclonal; red), vesicular GABA transporter (vGAT; green), and vesicular glutamate transporter-1 (vGLUT1; blue). (C, D) The insets magnify the dotted areas in the merged images. Scale bars: 10 μm (large images), 2 μm (inset image in C), and 1 μm (inset image in D). (E) Quantitative analysis of ARF1 colocalization with either vGLUT1- or vGAT-positive synaptosomes. After filtering the triple-channel microphotographs with the same lower threshold value, all images were converted to binary bitmaps. The total ARF1-immunolabeled area overlapping with that of vGLUT1 (purple) or vGAT (yellow) was calculated in percentage of total ARF1-positive area. For each channel pair, bars represent the mean overlap value ± standard error across 15 different images obtained from the same synaptosomal extraction.

Table 1.

Tissue sample characteristics. Diagnoses were established using DSM-IV criteria using all available information. Two subjects had a diagnosis of schizoaffective disorder. Post-mortem interval (PMI) and sample storage time were different between groups ($P < 0.001$, *t*-test). PMI was unavailable for one individual. Detailed sample information was previously described (Barakauskas et al., 2010)

	Controls mean (SD)	**Schizophrenia mean (SD)**
Age (years)	51.4 (18.8)	53.6 (12.1)
Postmortem interval (hours)	16.6 (7.1)	8.8 (3.2)
Sample storage time (weeks)	196 (77)	316 (74)
Brain pH	6.16 (0.33)	6.32 (0.22)
	n	*n*
Gender (Male: Female)	10:3	9:6
Smoker (yes:no:unknown)	8:4:1	9:4:2
Cause of death		
Cardiac	4	6
Accidental	6	2
Homicide	3	0
Gastrointestinal	0	3
Pulmonary	0	3
Undetermined	0	1

Table 2.

SNAP25 interactome in human control and schizophrenia ventromedial caudate samples. Protein names are listed as found in the European Bioinformatics Institute human International Protein Index (IPI) database. The mean Mascot score and mean number of discrete peptides used for protein identification are based on the total number of positive samples. Proteins identified were found in >2 samples and were identified using >1 discrete peptide. The sample number, average score and average peptide number reflects all samples in which the protein was identified, including samples that did not meet this threshold criteria. The number of individual samples (subjects) in which each protein was detected is given (*n*). The nominal *p*-value for comparison of proportions between groups is shown; only ARF1 was statistically significant after correction for 36 comparisons. Placing proteins in the mitochondria-associated group indicates a report with such an association, and does not imply a primary or exclusive mitochondrial origin (Boyken et al., 2013; Stauch et al., 2014; Demjaha et al., 2014; Laßek et al., 2015; Völgyi et al., 2015)

Protein	IPI#	UniProt	MASCOT score (mean)	Peptides (mean)	Con *n* (%)	Sch *n* (%)	Difference (*p*-value)
SNARE and related proteins							
SNAP25 Isoform SNAP25b of Synaptosome-associated protein 25	10470	P60880–1	373.9	8.3	13 (100)	15 (100)	
STX1A Isoform 1 of Syntaxin-1A	3370	Q16623	528.5	14.6	13 (100)	15 (100)	
STX1B Syntaxin-1B	410675	P61266	585.9	16.5	13 (100)	15 (100)	
VAMP2 Vesicle-associated membrane protein 2	553138	P63027	199.1	4.7	13 (100)	15 (100)	
SYT1 Synaptotagmin-1	9439	P21579	169.3	8.3	13 (100)	14 (93)	
STX7 Isoform 1 of Syntaxin-7	289876	015400	125.7	5.8	13 (100)	14 (93)	
STX12 Syntaxin-12	329332	Q86Y82	93.8	3.5	13 (100)	11 (73)	
STXBP1 Isoform 2 of Syntaxin-binding protein 1	46057	P61764–2	97.3	4.4	11 (85)	11 (73)	
SNAP25 Isoform SNAP25a of Synaptosome-associated protein 25	107625	P60880–2	259.4	7.4	10 (77)	10 (67)	
CPLX2 Complexin-2	12759	Q6PUV4	66.4	1.5	9 (69)	10 (67)	
VAMP1 Isoform 1 of Vesicle-associated membrane protein 1	12898	P23763	75.2	2.5	0 (0)	6 (40)	0.003
NSF Vesicle-fusing ATPase	6451	P46459	59.8	1.6	2 (15)	3 (20)	
STXBP1 Isoform 1 of Syntaxin-binding protein 1	84828	P61764–1	114.0	7.0	2 (15)	3 (20)	
SNAP29 Synaptosome-associated protein 29	32831	095721	65.2	1.2	2 (15)	3 (20)	
SYN1 Isoform IB of Synapsin-1	251507	P17600	59.2	2.6	0 (0)	5 (33)	0.007
Mitochondria-associated proteins							
VCP Transitional endoplasmic reticulum ATPase	22774	P55072	104.7	7.5	13 (100)	15 (100)	
RAB3A Ras-related protein Rab-3A	23504	P20336	100.6	3.4	12 (92)	13 (87)	
ATP5C1 Isoform Heart of ATP synthase subunit gamma, mitochondrial	395769	P36542	54.2	1.6	8 (62)	13 (87)	
TTYH1 Isoform 2 of Protein tweety homolog 1	10183	Q9H313	80.1	1.8	9 (69)	9 (60)	

Protein	IPI#	UniProt	MASCOT score (mean)	Peptides (mean)	Con *n* (%)	Sch *n* (%)	Difference (*p*-value)
ATP6AP1 V-type proton ATPase subunit S1	784119	Q15904	55.1	1.4	4 (31)	7 (47)	
ATP6V0D1 V-type proton ATPase subunit d 1	34159	P61421	68.6	1.9	5 (38)	6 (40)	
ATP5A1 ATP synthase subunit alpha, mitochondrial	440493	P25705	70.9	3.0	3 (23)	7 (47)	
HSPA8 Isoform 1 of Heat shock cognate 71 kDa protein	3865	P11142	71.4	3.5	6 (46)	4 (27)	
ARF1 ADP-ribosylation factor 1	215914	P84077	56.3	1.3	0 (0)	8 (53)	0.0004
PLP1 Isoform 1 of Myelin proteolipid protein	219661	P60601	117.7	2.8	2 (15)	4 (27)	
GAPDH Glyceraldehyde-3-phosphate dehydrogenase	219018	P04406	104.7	4.2	1 (8)	5 (33)	
RAB1A Isoform 1 of Ras-related protein Rab-1A	5719	P62820	60.8	2.0	2 (15)	3 (20)	
ATP5A1 cDNA FLJ54625, highly similar to ATP synthase subunit alpha, mitochondrial	471928	P25705	89.3	3.5	2 (15)	2 (13)	
MAP1B Microtubule-associated protein 1B	8868	P46821	55.0	1.3	1 (8)	3 (20)	
RAB8A Mel transforming oncogene variant (Fragment)	556414	Q59EP4	76.5	3.0	1 (8)	3 (20)	
ATP5B ATP synthase subunit beta, mitochondrial	303476	P06576	92.0	3.0	0(0)	4 (27)	0.02
ATP1B1 Isoform 1 of Sodium/potassium-transporting ATPase subunit beta-1	747849	P05026	69.3	1.3	1 (8)	2 (13)	
Other proteins							
Microfibrillar protein 2 (Fragment)	385143	Q9NP29	219.0	2.0	13 (100)	15 (100)	
Rheumatoid factor RF-ET9 (Fragment)	384404	Q9UL88	167.5	1.1	13 (100)	14 (93)	
FHL1 four and a half LIM domains 1 isoform 5	14398	Q13642	58.0	1.8	1 (8)	3 (20)	
RAB6B Ras-related protein Rab-6B	16891	Q9NRW1	76.3	2.7	0 (0)	3 (20)	0.04

Table 3.

SNAP25 interactome in human control and schizophrenia ventromedial caudate samples (this study SNAP25 IP1, and syntaxin IP) from an independent study of human brain (SNAP25 IP2 (Brinkmalm et al., 2014)) and from a study of presynaptic membranes and docked vesicles in rat, using an antibody detecting the presynaptic vesicle protein SV2 (Morciano et al., 2009)

Protein	SNAP25 IP1	Syntaxin IP	SNAP25 IP2	SV2IP
SNARE and related proteins				
SNAP25 Isoform SNAP25b of Synaptosome-associated protein 25	+	+	+	+
STX1A Isoform 1 of Syntaxin-1A	+	+	+	+
STX1B Syntaxin-1B	+	+	+	+
VAMP2 Vesicle-associated membrane protein 2	+	+	+	+
SYT1 Synaptotagmin-1	+	+	+	+
STX7 Isoform 1 of Syntaxin-7	+	−		
STX12 Syntaxin-12	+	−		
STXBP1 Isoform 2 of Syntaxin-binding protein 1	+	−	+	+
SNAP25 Isoform SNAP25a of Synaptosome-associated protein 25	+	−	+	+
CPLX2 Complexin-2	+	+	+	+
VAMP1 Isoform 1 of Vesicle-associated membrane protein 1	+	−	+	+
NSF Vesicle-fusing ATPase	+	−		+
STXBP1 Isoform 1 of Syntaxin-binding protein 1	+	−	+	+
SNAP29 Synaptosome-associated protein 29	+	−		
SYN1 Isoform IB of Synapsin-1	+	−	+	+
Mitochondria-associated proteins				
VCP Transitional endoplasmic reticulum ATPase	+	+		
RAB3A Ras-related protein Rab-3A	+	−	+	+
ATP5C1 Isoform Heart of ATP synthase subunit gamma, mitochondrial	+	−		+
TTYH1 Isoform 2 of Protein tweety homolog 1	+	−	+	+
ATP6AP1 V-type proton ATPase subunit S1	+	−		+
ATP6V0D1 V-type proton ATPase subunit d 1	+	−		+
ATP5A1 ATP synthase subunit alpha, mitochondrial	+	−	+	+
HSPA8 Isoform 1 of Heat shock cognate 71 kDa protein	+	−		+
ARF1 ADP-ribosylation factor 1	+	−		+
PLP1 Isoform 1 of Myelin proteolipid protein	+	−	+	+

Protein	SNAP25 IP1	Syntaxin IP	SNAP25 IP2	SV2IP
GAPDH Glyceraldehyde-3-phosphate dehydrogenase	+	–	+	+
RAB1A Isoform 1 of Ras-related protein Rab-1A	+	–	+	+
ATP5A1 cDNA FLJ54625, highly similar to ATP synthase subunit alpha, mitochondrial	+	–		+
MAP1B Microtubule-associated protein 1B	+	–		
RAB8A Mel transforming oncogene variant (Fragment)	+	–		
ATP5B ATP synthase subunit beta, mitochondrial	+	–		+
ATP1B1 Isoform 1 of Sodium/potassium-transporting ATPase subunit beta-1	+	–		+
Other proteins				
Microfibrillar protein 2 (Fragment)	+	+		
Rheumatoid factor RF-ET9 (Fragment)	+	–		
FHL1 four and a half LIM domains 1 isoform 5	+	–		
RAB6B Ras-related protein Rab-6B	+	–		+

Table 4.

Correlations between protein immunoreactivities in ventromedial caudate ($n = 28$)

	t-ARF1		UQCRC1		SNAP25		SNAP25-syntaxin interaction	
	r	***P*-value**	***r***	***P*-value**	***r***	***P*-value**	***r***	***P*-value**
ARF1–21	0.40	0.04	0.52	0.004	0.33	0.08	−0.39	0.04
ARF1–17			0.10	0.63	0.24	0.21	−0.19	0.34
UQCRC1					0.30	0.13	−0.23	0.24
SNAP25							−0.84	< 0.0001